ANOMALIES IN ACOUSTICAL PROPERTIES OF MERCURY NEAR THE LIQUID-GAS CRITICAL POINT

V. Kozhevnikov, University of Utah, Salt Lake City, UT 84112-0830.

Results of measurements of sound velocity and attenuation in fluid mercury at sub- and supercritical parameters of state (at temperatures up to 2100 K and pressures up to 190 MPa) are reviewed. Discussion is concentrated on anomalies observed near the liquid-gas critical point. These are: (1) Peculiarities in sound velocity and attenuation revealed in the close vicinity of the critical point, which can be attributed to an effect of fluctuation-induced forces in a prewetting film on the cell walls. (2) A maximum in sound attenuation in a region of a metal-dielectric transition, testifying for fluctuations accompanying the opening of a band gap. (3) A pressure dependence of sound velocity in superheated vapor, which changes sign near the critical temperature.

Keywords: acoustical properties, data, critical state, prewetting film, mercury.

INTRODUCTION.

One of the differences between metallic and dielectric liquids is that a liquid-gas transition in metals is simultaneously a metal-dielectric transition. Since the latter is associated with an obvious change in intermolecular bonding, it should lead to specific features in the bulk and surface thermophysical properties of metallic fluids compared

to dielectric fluids. The violation of the law of corresponding states in metals is one such feature. Near the critical point the metal-dielectric and liquid-gas transitions may occur separately. Possible phase diagrams for metallic fluids at high temperatures have been discussed in a pioneering paper by Landau and Zeldovich [1], which gave rise to many investigations of the physical properties of metallic fluids over a wide range of temperatures and pressures [2].

Most of the experiments have been performed with mercury because it has the lowest critical temperature among the metals; the critical parameters of mercury are (T_c, P_c) = (1764 K, 167 MPa) [3]. The properties which have been studied include equation of state, electrical conductivity, thermopower, optical reflectivity and extinction, NMR, Hall effect, sound velocity and attenuation (see Ref. 2 for references).

It was established that mercury heated under pressure becomes nonmetallic below the critical temperature at a density near 9 g/cm^3 which is about three halves of the critical density ρ_c = 5.9 g/cm^3 [4]. In this region significant alterations were found in electronic properties such as electrical conductivity [5], Hall effect [6], and Knight shift [7]. However no appreciable peculiarities in thermal properties have been observed. Probably a bending of the phase diagram mean diameter [4, 5, 8], a change in the slope of the density dependence of sound velocity [9-11], and a slight change in the nearest-molecular distance [12] could be mentioned as possible traces of the metal-dielectric transition in molecular properties. Anisimov and Zapridskii [13] interpreted the mean diameter bending as a result of the coupling of order parameters of the liquid-gas and metal-dielectric

transitions.

On the other hand strong anomalies have been unexpectedly found in thermopower in the supercritical region near the critical isochore and in saturated vapor at high temperature [14]. These anomalies, first revealed by Duckers and Ross [14a], have been investigated by different groups for more than twenty years, but no acceptable interpretation has been found. A mysterious feature of these anomalies was that their pattern was different in almost all the cited experiments. In a careful study by Neal and Cusack [14d] the possibility of a surface effect from mercury film absorbed on ceramic isolators was noted (the isolators were recrystallised alumina, translucent large crystallite alumina “Lucalox”, and beryllia).

In the 1980’s one more anomaly was revealed: an increase and maximum in the optical reflectivity at a sapphire-mercury interface when mercury was in the vapor phase near saturation [15]. The authors first interpreted the anomaly in reflectivity as a bulk clustering effect in dense mercury vapor. Later this interpretation was changed to a surface effect of a prewetting mercury film on sapphire [16], which was also supported by further experiments [17]. The prewetting phase diagram suggested in Ref. 16 looks similar to that found for dielectric fluids (see, for example, Ref. 18). Namely, the prewetting transition curve locates very close to the bulk coexistence curve and terminates below the bulk critical point. However, the proposed prewetting phase diagram for mercury on sapphire does not explain the supercritical thermopower anomalies as well as the maximum in optical reflectivity observed in Ref. 15(a-c).

To investigate the nature of the thermopower and optical anomalies we undertook acoustical experiments in 1993 - 97. In a first series of the measurements [19] anomalies in the sound velocity were found in the vapor phase off coexistence and at supercritical parameters of state. A phase region of the “acoustical” anomalies included the regions of the thermopower and optical anomalies. It was tentatively suggested that the acoustical anomalies had a cluster origin. After subsequent more detailed and precise measurements [3] it become clear that another, namely, a prewetting interpretation should be investigated. The latest experiments [20] established that the acoustical anomalies in the vapor phase and in the supercritical region originated from first-order prewetting phase transitions taking place in mercury vapor on molybdenum and niobium substrates. The prewetting phase diagram for mercury on the metallic substrates differs significantly from that for dielectric fluids. In particular, the prewetting transition curve is well separated from the liquid-gas coexistence line and continues above the bulk critical point. Similar conclusions have been made for prewetting in conducting liquid solutions K-KCl [21]. These results testify for the essential influence of distinct intermolecular potentials on the wetting behavior.

In this paper after a brief review of basic experimental features and results [3] we present some previously unpublished data, and discuss anomalies revealed in the close vicinity of the bulk critical point, in the region of the metal-dielectric transition, and in superheated mercury vapor near the critical temperature.

EXPERIMENTAL

The experiments have been performed with a pulsed phase-sensitive technique described in Ref. 22. The frequency of sound was 10 MHz. The sample length L was 2.1 mm. Uncertainty in the measurements of sound propagation time τ was 1 ns, which for the near-critical region corresponded to a fractional uncertainty on the order of 10^{-4}. Uncertainty in the data on sound velocity ($c = L/\tau$) did not exceed 0.4% [22]. Amplitudes of the acoustical signals have been recorded from an oscilloscope screen with an uncertainty of about 5%.

A cell, which design is shown in Fig. 1, was made from molybdenum. The cell had one buffer rod inserted into the cell body from below; the upper buffer rod was a part of the cell body. The cell was oriented vertically. The design and orientation of the cell were principally important for accurate measurements in the vicinity of the coexistence curve. Cells with two inserted buffer rods at any orientation are not appropriate for the measurements in this region, mostly because of strong convection flows in the sample destroying its equilibrium. In such cells peripheral parts out of the sample space determine a temperature interval for the existence of the convection flows. The same concerns cells whose design is similar to that shown in Fig.1 but employed horizontally, as well as vertical cells which have the sample reservoir above the sample space without special precautions [4]. (For more details see section “The cell for high-temperature measurements” in Ref. 22.) Difference in designs and orientations of the cells used in Refs. 14 and 15 is a probable reason of the discrepancies in data on aforementioned thermopower and reflectivity anomalies.

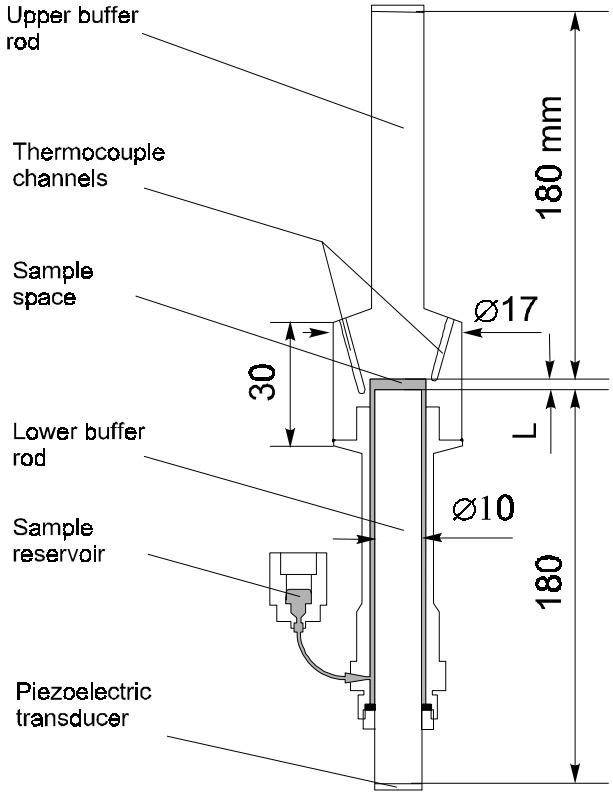

Fig.1. The cell.

The cell filled with mercury along with a heater was installed in a water-cooled high-pressure vessel. The heater consisted of three independently controlled sections made of 1 mm molybdenum wire with beryllia isolators. The vessel was filled with argon gas serving as a pressure-transmitting medium. All the measurements have been performed at steady state conditions.

The sample temperature was measured by two tungsten-rhenium thermocouples installed in channels of the cell body shown in Fig.1 (a wall thickness between the thermocouple junction and the sample was 0.5 mm). The thermocouples have been

calibrated according to the International Standard, and only this calibration was used for determination of the sample temperature [23]. A difference in the thermocouple readings ΔT mostly was within 2 K and did not exceed 8 K; a relative difference $\Delta T/T$ was on the order of 10^{-3}, where T is an average temperature over the sample. The difference ΔT was an order of magnitude smaller than the temperature interval of the acoustical anomalies. The pressure of the argon medium was transmitted to the sample through an open reservoir with liquid mercury. The gas pressure was measured by a Heise manometer with uncertainty 2 bar.

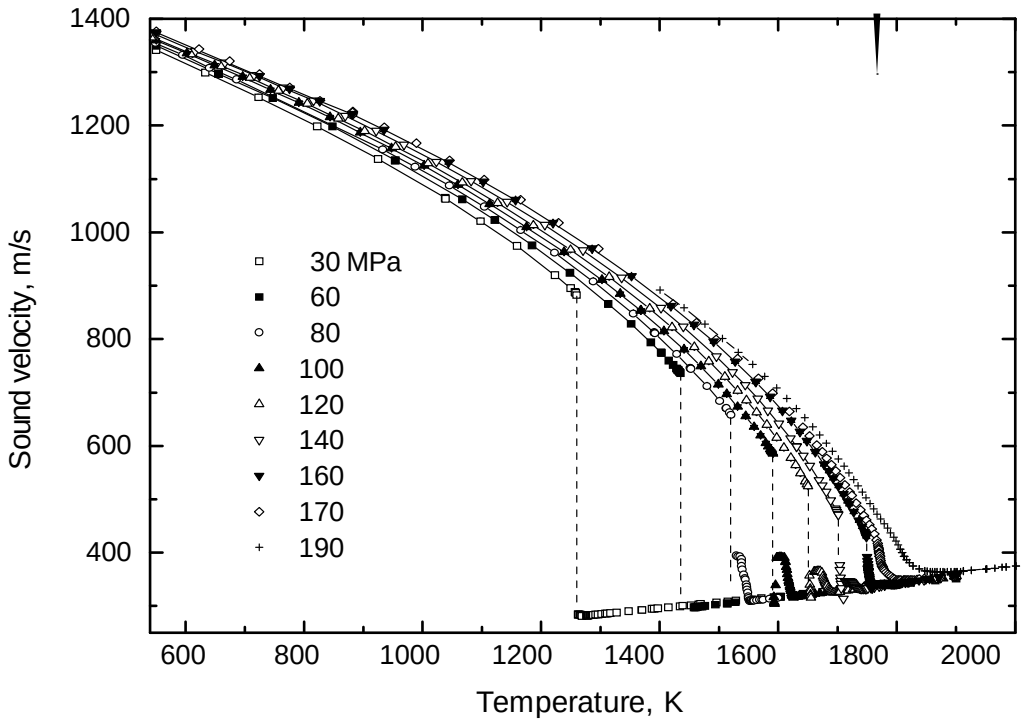

Fig. 2. Data on sound velocity in mercury measured at the indicated pressures. Arrow on the top corresponds to the critical temperature.

The mercury purity was 0.99999. Before filling, it was stored in sealed glass ampoules under vacuum. Impurities of Al, Be, Ca, Cu, Mo, Nb, and Si (total level on the order of 10^{-6} weight parts) were tested before the experiments. After the experiments with niobium cell [20a] the impurities were tested again for all these elements. After experiments with the molybdenum cell [3] we tested the level of Mo- and Cu-impurities. The tested mercury sample was in the molybdenum cell for more than two months, and was used for measurements of 26 isobars at temperatures up to 1900 K each. Results of the tests shown no contamination of the samples due to experiments.

DISCUSSION

The data on sound velocity and amplitude of the acoustical pulse transmitted through the sample in the molybdenum cell for the state parameters close to the critical point are shown in Fig. 3. The anomalous region at subcritical pressures locates between the coexistence curve (*A*-points) and *E*-points. The low-temperature bound of this region at supercritical pressures is less certain; it is somewhere near the critical isochore. (Location of the critical isochore is shown by a dashed line in Figs. 3(f-h).) The upper-temperature bound (E-point) is manifested as a short instability (or jump [20]) in the amplitude. At temperatures below E-point the curves for sound velocity exhibit a plateau. At $T > T_E$ sound velocity behaves as expected for normal superheated vapor; it is slowly increases with temperature. Crossing of the coexistence curve is determined on discontinuities in sound velocity and in the transmitted signal amplitude. The latter has a minimum on the vapor side of the curve. The deepest minimum is at the critical point,

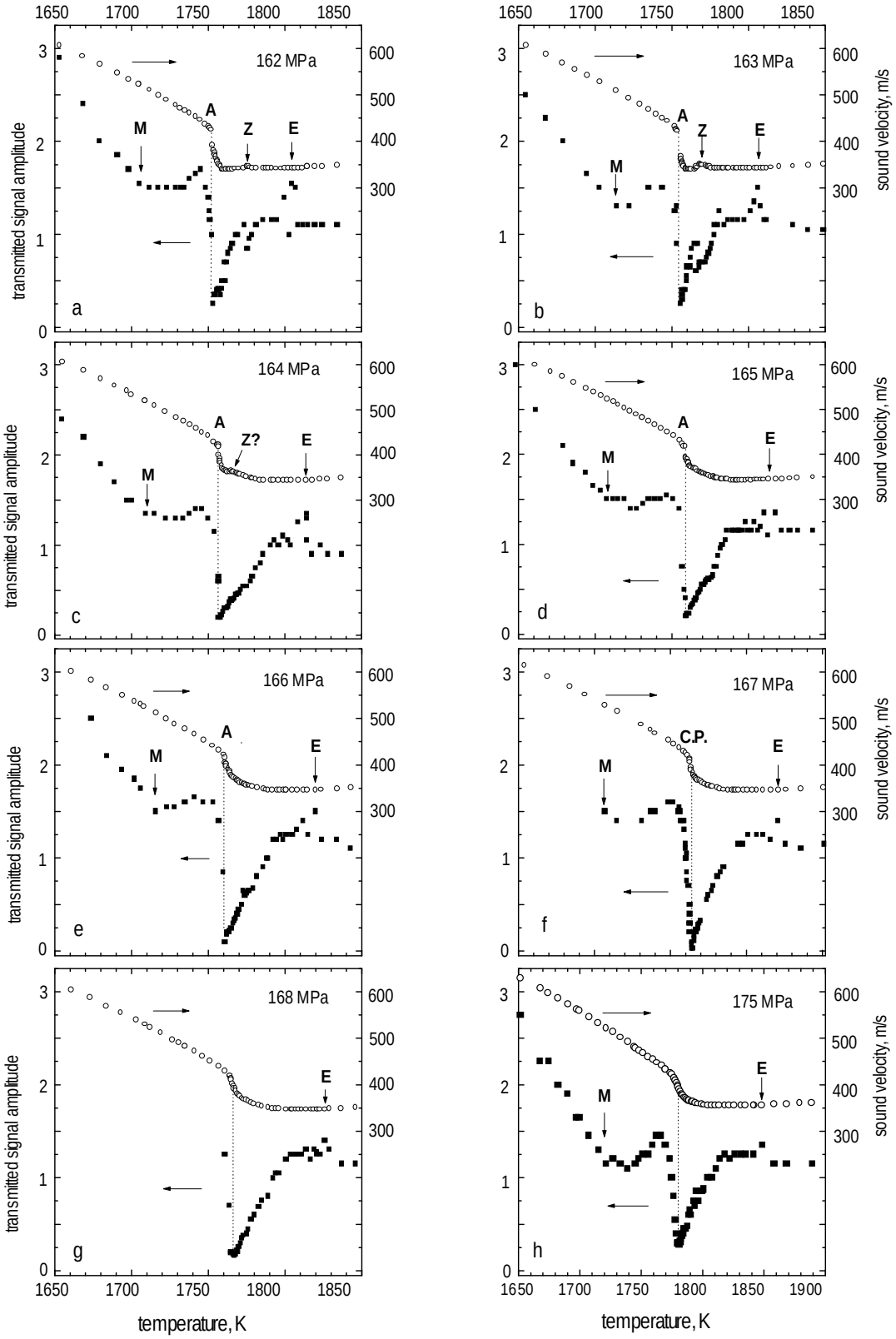
a
162 MPa
A
M
Z
E
b
163 MPa
A
Z
E
M
c
164 MPa
A
Z?
E
M
d
165 MPa
A
E
M
e
166 MPa
A
E
M
f
167 MPa
C.P.
E
M
g
168 MPa
E
h
175 MPa
E
M
transmitted signal amplitude
sound velocity, m/s
temperature, K
1650
1700
1750
1800
1850
1900
0
1
2
3
300
400
500
600

Fig. 3. Sound velocity and amplitude of the transmitted signal at constant pressures near the bulk critical point. The pressures are shown in the right top corners. Arbitrary units for amplitudes are the same in all the fragments. Letter *A* denotes the liquid-gas transition, *E* denotes the prewetting transition, *M* denotes the metal-dielectric transition, *C.P.* denotes the critical point, see the text for *Z*.

where the discontinuities disappear. Thus at such measurements the critical parameters are determined simultaneously from three specific features (two discontinuities plus depth of the minimum). This makes such data more reliable than that obtained from more traditional experiments, for example, from *PVT* (pressure-volume-temperature) measurements.

An increase of sound velocity near the low-temperature bound of the anomalous region can be explained as a consequence of the increasing prewetting film thickness near the liquid-gas coexistence (or near the critical isochore at supercritical pressures). From the data shown in Fig. 3 (see also Fig. 3 in Ref. 3) one may assume that the film thickness at coexistence increases with temperature. The same conclusion about the temperature dependence of the wetting film thickness has been recently made by Staroske et al. from direct ellipsometric measurements in a conducting K-KCl mixture [21b].

Near the critical point there is one more specific feature in the region between the *A*- and *E*-points, namely a small maximum in sound velocity accompanied by a minimum in the propagated signal. It is marked by the letter *Z* in Figs. 3(a-c). Temperature of the *Z*-point approaches the critical temperature as the pressure approaches the critical pressure.

The *Z*- peculiarity is explicitly seen at pressures 162 and 163 MPa, and is partially masked by the rising part of the sound velocity curve at 164 MPa. This allows us to speculate that this feature could be seen in the other near-critical isobars, if it was not suppressed by the stronger effect of the prewetting film growth.

A possible interpretation of the *Z*-peculiarity might be as follows. When a prewetting film adsorbed on a solid substrate is brought to the state parameters close to the bulk critical point, the critical fluctuations developed in the film are spatially restricted by its thickness. This should lead to the appearance of fluctuation-induced forces [24-26], also known as Casimir forces. This forces tend to alter the film thickness, which otherwise is determined by a competition between the film - substrate molecular interaction and gravitational potential energy [27]. Recently the critical Casimir effect has been studied in the wetting films of binary liquid mixtures on an oxidized silicon wafer [28] and in helium films on copper substrates [29]. A theory predicts [30] that the film thickness d in the presence of the critical fluctuations is determined by a scaling function $\vartheta(d/\xi)$, where ξ is the correlation length of fluctuations. ϑ can be also expressed through an argument $x = td^{1/\nu}$, where t is reduced temperature with respect to the critical point and ν is the critical exponent of the correlation length. This means that the temperature, at which the fluctuation-induced forces are maximum in the external field, is shifted relative to the critical temperature, and this shift decreases when the system approaches the critical point [29].

Since the prewetting mercury film on the metallic substrate exists near the bulk critical point, the Casimir effect should appear in its vicinity. The closer the system is to the critical point, the stronger is the anticipated effect. For our case this means that when the pressure of the isobars approaches the critical pressure, the temperature of the "Casimir-peculiarity" should approach the critical temperature and its magnitude should increase. This is what we have for the *Z*-points in Figs. 3(a-c). The simultaneous minimum in the amplitude of the transmitted signal is explained by additional attenuation of sound coming through the film on the side wall caused by the critical fluctuations in the film. In this region the received signal comes from a superposition of signals transmitted through the bulk sample and the film. Assuming that the fluctuation-induced forces originate the *Z*-peculiarity, one may conclude that these forces thick the mercury film adsorbed on the molybdenum substrate. Note, that Casimir forces thin a helium film on copper near the λ-point [29], and thick the films in the experiments with binary liquids [28].

All the currently available information on the *Z*-peculiarity is presented in Figs. 3(a-c); it is apparently too small for quantitative analysis. Additional more detailed experiments are required. These, in particular, can be acoustic measurements performed with a smaller step in pressure on metallic cells with different acoustic path lengths. It is also very interesting to carry out simultaneous acoustic and optical measurements in this region with a transparent (sapphire) cell. Electrical conductivity measurements similar to that done by Borzhievskii et al. with cesium [31] can also be very informative.

Another specific feature seen in Figs. 3 is a minimum on the liquid side of the amplitude curves (or at densities higher than the critical density at supercritical pressures). In this region the sample is uniform and therefore this feature is a bulk property of mercury. The minimum is denoted by the letter *M*. Position of *M* corresponds to a density of 9 g/cm^3 at which the metal-dielectric transition takes place. Similar dependencies measured at pressures 100 and 120 MPa [20] exhibit no minimum. Isobars 100 and 120 MPa do not cross isochore 9 g/cm^3. For this reason we conclude that this minimum originates from the metal-dielectric transition. Because the amplitude of the transmitted signal depends on sound attenuation, the minimum in the transmitted signal should be associated with a maximum in sound attenuation [22]. Data on sound attenuation for isobar 162 MPa are shown in Fig. 4. One can see that a "gentle" minimum in Fig 3a corresponds to a well-shaped maximum in the sound attenuation coefficient, which position perfectly coincides with the intersection of isochore 9 g/cm^3. A similar maximum in sound attenuation was recently found by Kohno and Yao [32].

A sound attenuation maximum at the metal-dielectric transition can be interpreted as an effect of fluctuations caused by an opening of the band gap and corresponding change in intermolecular bonding. If so, existing models of the metal-dielectric transition in mercury (see, for example, Refs. 33) should be modified to incorporate this effect. The fluctuations may lead to specific features in high order derivatives of a thermodynamic potential of the system, resembling a thermodynamic phase transition of a higher than second order.

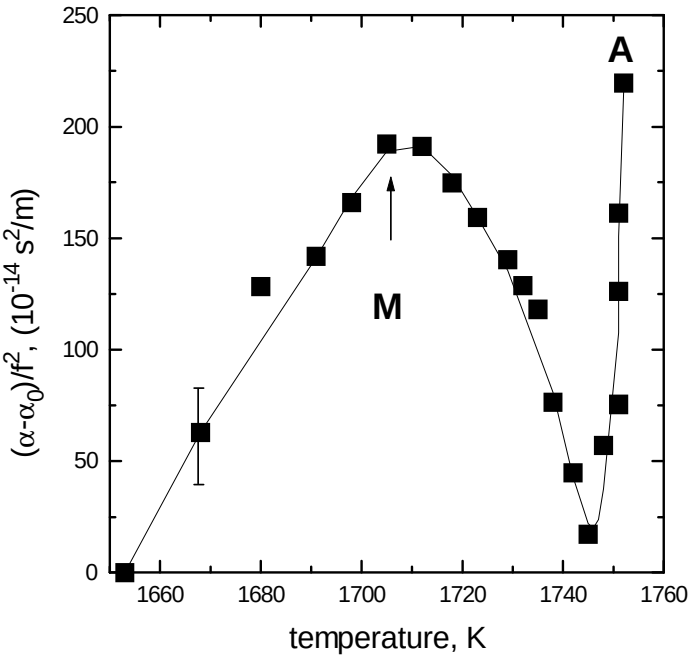

Fig. 4. A change of sound attenuation in liquid mercury at 162 MPa (after Ref. 22). For *A* and *M* points see captions of Fig.3.

A hint on the possibility of such a scenario comes from the aforementioned inflection in the density dependence of sound velocity near 9 g/cm^3. In Fig. 5 the sound velocity data of Fig.2 are presented as function of density. Tables on density by Gotzlaff [8a] have been used for this plot. All the sound velocity data collapse to a nearly single density dependence, whose slope significantly changes near 9 g/cm^3. This implies a maximum in a fourth order volume derivative of the internal energy of fluid mercury [10].

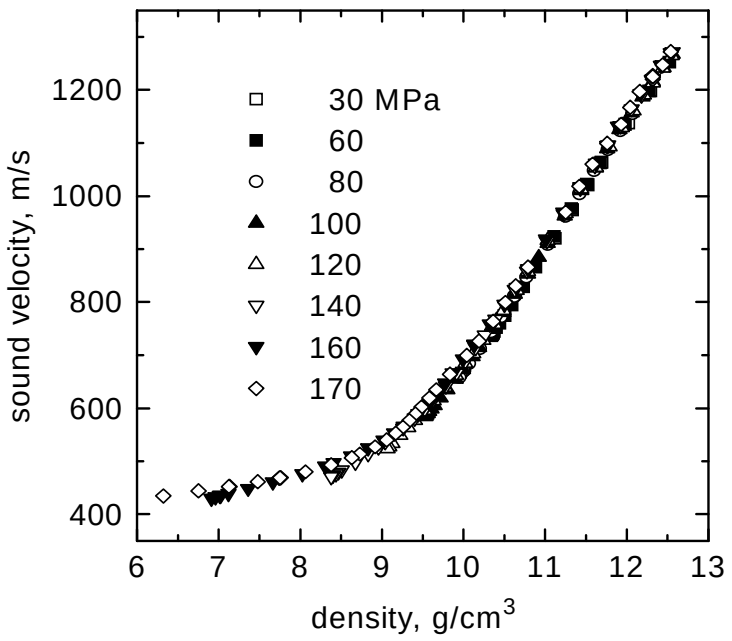

Fig. 5. Sound velocity in mercury versus density.

The latest feature revealed in the acoustic properties of near-critical mercury concerns the behavior of sound velocity in superheated mercury vapor at $T > T_E$. In this region the sample was uniform again. So we discuss bulk properties of the mercury vapor. The experimental data are shown in Fig. 6; numerical values are given in the Appendix. A curve of sound velocity for an ideal monatomic mercury gas ($c = (\gamma RT/\mu)^{1/2}$, where $\gamma \equiv C_p/C_v = 5/3$ is the ratio of heat capacities, R is the universal gas constant, and μ is the molar mass) is also shown in this figure. A curve for a diatomic ideal gas lies essentially lower.

The sound velocity behavior in a normal vapor basically agrees with what was found in our earlier experiment [19a]. It shows that the vapor mainly consists of

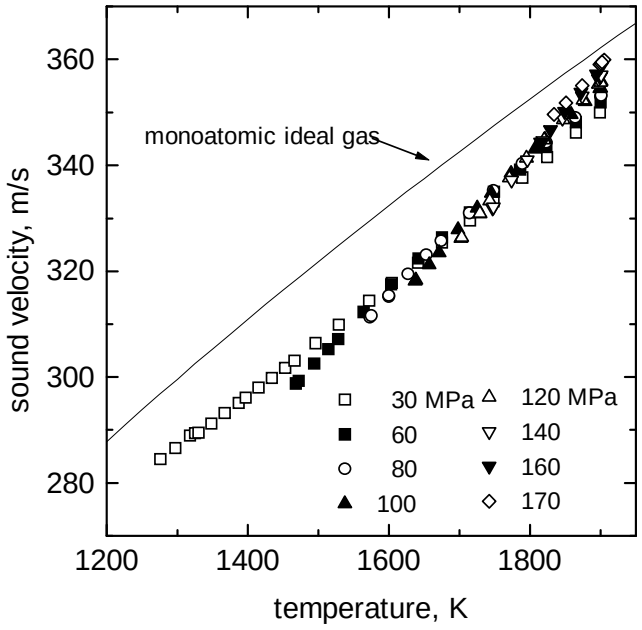

Fig. 6. Sound velocity in mercury vapor at constant pressures.

monatomic molecules, which increase in number with temperature. Isobar 30 MPa goes nearly parallel to the ideal gas curve. This may lend support for a minor change in composition at low pressure. However we should note that the data at 30 MPa are less reliable because of the largest mismatch in acoustical impedances of the sample and the buffer rods at this pressure. (This mismatch resulted in very low amplitude of the transmitted signal, and did not allow measurements at lower pressures.) What was not noticed in Ref. 19a, but is explicitly seen in Fig. 6, is a weak (3% at 1900 K) but distinct pressure dependence of sound velocity. This represents a signature of a nonideality of the mercury vapor. It is interesting that the pressure dependence at relatively low

temperatures is negative (sound velocity decreases with pressure) whereas at higher temperatures it is positive. The sign changes near the critical temperature.

A qualitatively similar behavior is anticipated from the van der Waals model. In this model sound velocity squared, $c^2 = \gamma(\partial P/\partial \rho)_T$, can be written as

$$c^2 = \frac{\gamma}{\mu}\left[\frac{RT}{(1 - b\rho/\mu)^2} - \frac{2a\rho}{\mu}\right] \qquad (1)$$

where ρ is the mass density, and a and b are intermolecular and volume constants of the van der Waals' equation, respectively.

Taking into account that in this model the critical temperature and density are $T_c = 8a/27Rb$ and $\rho_c = \mu/3b$, then equation (1) takes form

$$c^2 = \frac{\gamma R}{\mu}\left[\frac{T}{(1 - x)^2} - \frac{27\, T_c\, x}{4}\right] \qquad (2)$$

where $x = \rho/3\rho_c$.

Thus at low temperatures ($T < T_c$) and correspondingly small densities ($x \ll 1$), the behavior of sound velocity at constant temperature is governed by the second term of these equations, which decreases sound velocity with density (or pressure). At high temperatures and densities the slope sign changes. The model predicts that at the critical temperature the slope changes sign at about $1.5\rho_c$. In real mercury vapor this takes place at densities below ρ_c. Therefore experimental data on sound velocity can be used to develop a more realistic model for intermolecular interaction in a dense metallic vapor.

CONCLUSIONS.

We have discussed anomalies revealed in the acoustical investigation of the bulk and surface properties of fluid mercury near its liquid-gas critical point. It was shown that peculiarities in sound velocity and attenuation in the close vicinity of the critical point might be associated with the effect of the fluctuation-induced forces in the prewetting mercury film adsorbed on a rigid molybdenum substrate. Additional more careful and detailed measurements are possible and desired for quantitative comparison of this observation with theoretical predictions. The film properties should change in the supercritical region. Behavior of the adsorbed metallic film at supercritical parameters of state remains an intriguing puzzle of this field.

It was shown that a metal-dielectric transition in bulk liquid mercury is accompanied by a maximum in sound attenuation. This result provides new insight into the metal-dielectric transition in expanded metals. It is also desirable to perform more careful investigations of this anomaly. In particular, it is interesting and instructive for theory to investigate dispersion of the acoustic properties of mercury in this region.

A fine pattern of sound velocity in superheated mercury vapor differs from that expected for an ideal gas mixture of mono- and multiatomic molecules. The data obtained may be used to compose a realistic model for the equation of state and intermolecular interaction in dense metallic vapor at sub- and supercritical parameters of state.

ACKNOWLEDGES.

I am grateful for active interest and encouragement of Johanna M.H. Levelt Sengers, Michael E. Fisher, Dmitrii I. Arnold, Milton Cole, Moses H.W. Chan, and Salim P. Naurzakov. Help of John M. Viner have been greatly appreciated.

This work was partly supported by a research grant of the University of Utah.

APPENDIX.

Experimental data on sound velocity in superheated mercury vapor (T, K; c, m/s).

P = 30 MPa

1276	284
1297	287
1318	289
1325	289
1330	289
1348	291
1367	293
1387	295
1397	296
1415	298
1434	300
1453	302
1466	303
1496	306
1529	310
1572	314
1604	318
1641	322
1675	325
1715	330
1748	333
1789	338
1824	341
1865	346
1899	350

P = 60 MPa

1468	299
1472	299
1494	303
1514	305
1528	307
1564	312
1603	318
1642	322
1675	326
1715	331
1749	335
1786	339
1823	343
1865	348
1900	352

P = 80 MPa

1573	311
1575	312
1600	315
1627	319
1653	323
1674	326
1714	331
1748	335
1789	340
1823	344
1864	349
1900	353

P = 100 MPa

1637	318
1638	318
1657	321
1671	323
1698	328
1725	332
1745	335
1773	339
1807	343
1821	345
1858	350
1878	352
1900	355

P = 120 MPa

1702	326
1703	326
1729	331
1743	333
1771	338
1795	341
1820	345
1847	349
1875	352
1897	355
1901	356

P = 140 MPa

1747	332
1748	332
1774	337
1796	341
1818	345
1846	349
1874	353
1897	356
1900	357

P = 160 MPa

1815	344
1829	347
1849	350
1872	354
1894	357
1901	359

P = 170 MPa

1834	350
1851	352
1874	355
1899	359
1902	359
1905	360

REFERENCES

1. L.D. Landau and Ya.B. Zeldovich, Acta Phys. Chem. USSR, 18 (1943) 194-196.
2. F. Hensel and W.W. Warren, Jr., Fluid Metals, Princeton University Press, Princeton, 1999.
3. V. Kozhevnikov, D. Arnold, E. Grodzinskii, and S. Naurzakov, Fluid Phase Equilibria, 125 (1996) 149-157.
4. I.K. Kikoin, A.P. Senchenkov, S.P. Naurzakov, and E.B. Gelman, Report IAE-2310, Kurchatov Institute of Atomic Energy, Moscow, 1973.
5. I.K. Kikoin and A.P. Senchenkov, Fizika Metallov i Metallovedenie, 24 (1967) 843-855 (transl.: Phys. Met. Metall., 24 (1967) 74-89).
6. U. Even and J. Jortner, Phys. Rev. Lett., 28 (1972) 31-34.
7. U. El-Hanany and W.W. Warren, Jr., Phys. Rev. Lett., 34 (1975) 1276-1279.
8. W. Gotzlaff, Thesis, Marburg University, 1988; W. Gotzlaff, G. Shonherr, and F. Hensel, Z. Phys. Chem. N.F., 156, (1988) 219-223.
9. K. Susuki, M. Inutake, and S. Fujiwaka, IPPJ-310 (1977); M. Inutake, K. Susuki, and S. Fujiwaka, J. Phys. (Paris), 40 (1979) C7-685 - C7-686.
10. V.F. Kozhevnikov, D.I. Arnold, and S.P. Naurzakov, Intern. J. Thermophys., 16 (1995) 619-626.
11. M. Yao, K. Okada, T. Aoki, and H. Endo, J. Non Crystal. Solids, 205-207 (1996) 274-277.
12. K. Tamura, M. Inui, I. Nakaso, Y. Oh'ishi, K. Funakoshi, and W. Utsumi, J. Phys: Condens. Matter, 10 (1998) 11405-11417.

13. M. Anisimov, Critical Phenomena in Liquids and Liquid Crystals, Gordon and Breach, Amsterdam, 1991.
14. (a) L.J. Duckers and R.G. Ross, Phys. Lett., 38A (1972) 291-292; (b) V.A. Alekseev, A.A. Vedenov, V.G. Ovcharenko, Yu. F. Ruzhkov, and A.N. Starostin, JETP Letters, 16 (1972) 49-52; (c) K. Tsuji, M. Yao, and H. Endo, J. Phys. Soc. Jpn., 42 (1977) 1594 - 1600; (d) F.E. Neal and N.E. Cusack, J. Phys. F.: Metal Phys., 9 (1979) 85-94; (e) V.A. Alekseev, V.G. Ovcharenko, and Yu.F. Ruzhkov, J. Phys. (Paris), 41 (1980) C8-91 - C8-93; (f) M. Yao and H. Endo, J. Phys. Soc. Jpn., 51 (1982) 1504 - 1509; (g) M. Yao, K. Takehana, and H. Endo, J. Non-Cryst. Solids 156-158 (1993) 807-811.
15. (a) W. Hefner, R.W. Schmutzler, and F. Hensel, J. Phys. (Paris), 41 (1980) C8-65 - C8-65; (b) W. Hefner and F. Hensel, Phys. Rev. Lett., 48 (1982) 1026-1028; (c) W. Hefner, Thesis, University of Marburg, 1980; (d) M. Yao, H. Uchtmann, and F. Hensel, Surface Science, 156 (1985) 465-459.
16. M. Yao and F. Hensel, J. Phys. Condens. Matter, 8 (1996) 9547-9550.
17. Y. Ohmasa, Y. Kajihara, H. Kohno, Y. Hiejima, and M. Yao, J. Phys.: Condens. Matter, 12 (2000) A375-A381.
18. J.E. Rutledge and P. Taborek, Phys. Rev. Lett., 69 (1992) 937-940; E. Cheng, G.Mistura, H.C. Lee, M.H.W. Chan, M.W. Cole, C. Carraro, W.F. Saam, and F. Toigo, Phys. Rev. Lett., 70 (1993) 1854-1857; B. Evans and M. Chan, Phys. World, April 1996, 48-52.

19. (a) V.F. Kozhevnikov, S.P. Naurzakov, and D.I. Arnold, J. Moscow Phys. Soc., 3 (1993) 191-201; (b) V.F. Kozhevnikov, D.I. Arnold, and S.P. Naurzakov, J. Phys.: Condens. Matter, 6 (1994) A249-A254.
20. (a) V.F. Kozhevnikov, D.I. Arnold, S.P. Naurzakov, and M.F. Fisher, Phys. Rev. Lett., 78 (1997) 1735-1738; (b) V.F. Kozhevnikov, D.I. Arnold, S.P. Naurzakov, and M.F. Fisher, Fluid Phase Equilibria, 150-151 (1998) 625-632.
21. (a) H. Tostmann, D. Nattland, and W. Freyland, J. Chem. Phys., 104 (1996) 8777-8785; (b) S. Staroke, D. Nattland, and W. Freyland Phys. Rev. Lett., 84 (2000) 1736-1739.
22. V.F. Kozhevnikov, D.I. Arnold, M.E. Briggs, S.P. Naurzakov, J.M. Viner, and P.C. Taylor, J. Acoust. Soc. Am., 106 (1999) 3424-3433.
23. In some works (see, for example Refs. 8 and 32) readings of a standard temperature gage are corrected with respect to data on pressure dependence of the boiling temperature, which is believed are more accurate. These corrections testify about differences between the gage and sample temperatures. Such corrections (or recalibrations) can be valid for measurements at the coexistence curve itself, but they are not appropriate away of this curve, because the aforementioned difference depends on pressure.
24. M.E. Fisher and P.G. de Gennes, C.R. Acad. Sci. Ser.B., 287 (1978) 209- 213.
25. M.P. Naghtingale and J.O. Indekeu, Phys. Rev. Lett., 54 (1985) 1824-1827.
26. M. Krech, J. Phys.: Condens. Matter, 11 (1999) R391-R412.
27. E. Cheng and M.W. Cole, Phys. Rev. B, 38 (1988) 987-995.

28. A. Mukhopadhyay and B.M. Law, Phys. Rev. Lett., 83 (1999) 772-775.

29. R. Garcia and M.H.W. Chan, Phys. Rev. Lett., 83 (1999) 1187-1190.

30. V. Privman and M. Fisher, Phys. Rev. B, 30 (1984) 322-327.

31. A.A. Borzhievskii, V.A. Sechenov, and V.I. Khorunzhenko, Tepofiz. Vys. Temp., 26 (1988) 722-726.

32. H. Kohno and M. Yao, J. Phys.: Condens. Matter, 11 (1999) 5399-5413.

33. J.R. Franz, Phys. Rev. Lett., 57 (1986) 889-892.